

## Activation of Akt/FKHR in the medulla oblongata contributes to spontaneous respiratory recovery after incomplete spinal cord injury in adult rats



M.S. Felix <sup>a,b,c,1</sup>, S. Bauer <sup>a,b,c,1</sup>, F. Darlot <sup>c</sup>, F. Muscatelli <sup>a,b</sup>, A. Kastner <sup>c,d</sup>, P. Gauthier <sup>c,e</sup>, V. Matarazzo <sup>a,b,c,\*</sup>

<sup>a</sup> Aix-Marseille Université, INMED UMR 901, 13273 Marseille, France

<sup>b</sup> INSERM, UMR 901, 13273 Marseille, France

<sup>c</sup> Aix-Marseille Université, CNRS, CRN2M UMR 6231, 13397 Marseille, France

<sup>d</sup> Aix-Marseille Université, PPSN EA 4674, 13013 Marseille, France

<sup>e</sup> Aix-Marseille Université, CNRS, LNIU UMR 7260, 13331 Marseille, France

### ARTICLE INFO

#### Article history:

Received 2 February 2014

Revised 25 April 2014

Accepted 17 May 2014

Available online 27 May 2014

#### Keywords:

Cervical hemisection

Diaphragm

FOXO1A

FKHR

P-Akt

Plasticity

### ABSTRACT

After incomplete spinal cord injury (SCI), patients and animals may exhibit some spontaneous functional recovery which can be partly attributed to remodeling of injured neural circuitry. This post-lesion plasticity implies spinal remodeling but increasing evidences suggest that supraspinal structures contribute also to the functional recovery. Here we tested the hypothesis that partial SCI may activate cell-signaling pathway(s) at the supraspinal level and that this molecular response may contribute to spontaneous recovery. With this aim, we used a rat model of partial cervical hemisection which injures the bulbospinal respiratory tract originating from the medulla oblongata of the brainstem but leads to a time-dependent spontaneous functional recovery of the paralyzed hemidiaphragm. We first demonstrate that after SCI the PI3K/Akt signaling pathway is activated in the medulla oblongata of the brainstem, resulting in an inactivation of its pro-apoptotic downstream target, forkhead transcription factor (FKHR/FOXO1A). Retrograde labeling of medullary premotoneurons including respiratory ones which project to phrenic motoneurons reveals an increased FKHR phosphorylation in their cell bodies together with an unchanged cell number. Medulla infusion of the PI3K inhibitor, LY294002, prevents the SCI-induced Akt and FKHR phosphorylations and activates one of its death-promoting downstream targets, Fas ligand. Quantitative EMG analyses of diaphragmatic contractility demonstrate that the inhibition of medulla PI3K/Akt signaling prevents spontaneous respiratory recovery normally observed after partial cervical SCI. Such inhibition does not however affect either baseline contractile frequency or the ventilatory reactivity under acute respiratory challenge. Together, these findings provide novel evidence of supraspinal cellular contribution to the spontaneous respiratory recovery after partial SCI.

© 2014 Elsevier Inc. All rights reserved.

### Introduction

After partial injury, the adult central nervous system (CNS) is still capable of significant post-lesion plasticity accompanied by a certain degree of functional recovery. This includes partial spinal cord injuries (SCIs) where, despite an extensive axotomy, plasticity allows the descending drive to re-establish brain inputs on spinal circuits (Rossignol and Frigon, 2011). At the spinal level, post-lesional plasticity processes mainly consist of collateral sprouting of both spared and

injured neurons enhanced connectivity of spared neurons and activation of quiescent networks (Steward et al., 2008). This remodeling had been demonstrated for the corticospinal, the reticulo-spinal locomotor and the bulbospinal respiratory tracts (Ballermann and Fouad, 2006; Bareyre et al., 2004; Baussart et al., 2006; Darlot et al., 2012; Ghosh et al., 2010; Kyoto et al., 2007; Polentes et al., 2004; Steward et al., 2008) and results in partial spontaneous recovery of locomotor or autonomic activities like respiratory function (Lane et al., 2008, 2009; Raineteau and Schwab, 2001; Rossignol et al., 2008; Vinit and Kastner, 2009). A great deal of effort has been expended in studying the potential cell-signaling pathways that operate for spontaneous recovery after partial SCI, which has led to the functional identification of numerous molecular factors of neuroplasticity, neuroprotection, axonal outgrowth... (Hulsebosch, 2002). Much of this knowledge has been addressed at the lesion site of the spinal cord, but the contribution of supraspinal structures in recovery has yet to receive in-depth attention.

\* Corresponding author at: Aix-Marseille Université, Institut de Neurobiologie de la Méditerranée (INMED), INSERM UMR 901, 163 route de Luminy, BP13, 13273 Marseille, France. Fax: +33 491 828101.

E-mail address: [valery.matarazzo@inserm.fr](mailto:valery.matarazzo@inserm.fr) (V. Matarazzo). Available online on ScienceDirect ([www.sciencedirect.com](http://www.sciencedirect.com)).

<sup>1</sup> Equal contribution.

Indeed, in both vertebrates and invertebrates, evidence is emerging that brain compensatory mechanisms also contribute to recovery from SCI (Nishimura and Isa, 2009, 2012; Reimer et al., 2013). However, the molecular bases of these compensatory mechanisms are poorly characterized. In the present study, we hypothesized that, in addition to the cell-signaling pathways sustaining post-lesional plasticity in the spinal cord, supraspinal molecular events may also participate to the recovery. In order to decipher potential supraspinal molecular factors, we used a model of post-lesional spontaneous recovery: a lateral incomplete hemisection of the rat cervical spinal cord (Vinit et al., 2007). This type of mild cervical injury severs part of the descending motor tracts including the ipsilateral bulbospinal respiratory premotoneurons originating from the medulla oblongata of the brainstem and driving the cervical phrenic motoneuron pool (Krassioukov, 2009). This experimental model of SCI has been shown to be a relevant model to study post-lesional plasticity of the respiratory descending tract and recovery of respiratory function (Darlot et al., 2012; Lane et al., 2009). Indeed, while such partial injury instantly abolishes the ipsilateral hemidiaphragm motor activity, spontaneous neural plasticity allows the paralyzed hemidiaphragm to recover within a few weeks (Goshgarian, 2003, 2009; Lane et al., 2008, 2009; Vinit and Kastner, 2009; Vinit et al., 2008). Although the plasticity of the neural circuitry that sustains this extensive respiratory recovery is well documented, the contribution of supraspinal cell-signaling mechanisms is unknown.

Here, using this model of postlesional plasticity after SCI, we first screened for activated transcription factors with the purpose of finding medulla cell-signaling pathway candidates that could be switched on during the spontaneous respiratory recovery period. Subsequently we directly assessed the functional contribution of the medulla oblongata in motor recovery of the diaphragm by combining electrophysiology and pharmacological inhibition in an *in vivo* longitudinal experiment. The present study provides novel evidence of a role of an endogenous supraspinal contribution in the time-dependent spontaneous functional recovery of the respiratory system after incomplete cervical hemisection.

## Material and methods

### Animal care and experimental groups

Young adult female Sprague–Dawley rats (250–300 g) were handled and cared in accordance with the *Guide for the Care and Use of Laboratory Animals* (N.R.C., 2011) and the European Communities Council Directive of September 22th 2010 (2010/63/EU, 74). Experimental protocols were approved by the institutional Ethical Committee guidelines for animal research with the accreditation no. C13-055-6 from the French Ministry of Agriculture. V. Matarazzo permit number # 13.305. All efforts were made to minimize the number of animals used and their suffering. A total of 50 rats were used in this study. 38 of them were submitted to C2 partial hemisection and housed for different post-lesion times. 12 animals went through the same surgery procedures but were not submitted to spinal cord injury and are referred as sham uninjured (see Supplementary Fig. S1).

### Spinal cord injury surgical procedures

Animals were anesthetized by an intraperitoneal (i.p.) injection using a mixture of ketamine (80 mg/kg, Imalgène 1000, Virbac) and xylazine (20 mg/kg, Bayer). Briefly, the rats were placed in a surgery system and their body temperature was maintained between 36.5 °C and 37.5 °C. Head and neck were shaved and washed with betadine and skin and muscles covering the second vertebrae were retracted. A laminectomy of the dorsal C2 vertebra was performed and the dura mater was cut and put aside. The left side of the spinal cord was transected laterally at the C2 segmental level with a microscalpel, just caudally to the C2 dorsal roots. After injury, muscles and skin were sutured, and animals received morphine (0.1 mg/ml, Lavoisier, France),

tetramycine (8%, Pfizer, France) and glucose (5%, Lavoisier, France) during the first 24 h. After surgery, animals were housed singly in temperature controlled conditions with a 12 h light/dark cycle; with access to food and water *ad libitum*.

### Nuclear extract and TranSignal™ DNA/protein array

Medulla nuclear extracts were isolated using the Affymetrix nuclear extraction kit (Affymetrix, Panomics, Redwood, CA) and according to the manufacturer's instructions. Briefly, cerebellum was removed in order to visualize the obex, area postrema and the 4th ventricle. A first coronal section was performed at the obex (bregma – 14.5 mm) and a second one 1.5 mm rostral to obex (bregma – 13.0 mm). Such anatomical landmarks allowed accurate dissection of regions of interest encompassing the rostral ventral respiratory group (VRG) and the raphe pallidus. Tissues were weighed and thawed in liquid nitrogen. First, Buffer A Working Reagent was added and tissues were homogenized with an electric mixer at 4 °C. After incubation at 4 °C for 15 min, samples were centrifuged at 850 g, at 4 °C for 10 min. Supernatants were removed and pellets were resuspended in buffer A. Samples were centrifuged again at 14,000 g, at 4 °C for 3 min. Pellets were resuspended in Buffer B Working Reagent to lyse nuclei, vortexed, then incubated for 1 h at 4 °C with gently shaking samples every 20 min. Finally, one last centrifugation at 14,000 g, at 4 °C for 5 min was performed to collect supernatants containing nuclear extracts. Total protein concentration of each sample was determined by BCA protein assay kit (Pierce Biotechnology, Rockford, IL, USA).

Activity of 20 transcription factors was profiled using the cell growth TranSignal™ DNA/protein array (Affymetrix, Panomics, Redwood, CA) and according to the manufacturer's instructions. Briefly, for each condition (uninjured, 7 dpi and 90 dpi rats), a total of 25 µg nuclear extract was mixed with biotin-labeled DNA binding probes (a set of 20 DNA binding oligonucleotides corresponding to the consensus sequences of 20 transcription factors, respectively) to allow the formation of DNA/protein complexes, which were then separated from the unbound probes by a spin column. After elution of the DNA/protein complexes, they were denatured to liberate the free probes, and used to hybridize the TranSignal Array that had been spotted with the consensus-binding sequences of the 20 transcription factors. Membranes were washed, treated with Streptavidin–AP conjugate for 30 min and re-washed. Signal on the membrane was detected using the SuperSignal West-Pico Chemiluminescent Substrate (Pierce, Thermo Scientific, France). Autoradiographic films were scanned and dot intensities from the generated digital images were quantified using gel tool Image J® (NIH, Bethesda, MD, USA). An arbitrary 2-fold change cutoff was established for significant difference in transcription activity between uninjured and injured conditions.

### Immunoblotting

Rats were sacrificed by decapitation, cervical spinal cord C4 and medulla were immediately dissected and snap-frozen in liquid nitrogen and stored at –80 °C until protein extraction. Tissues were homogenized on ice for 45 min in 50 µl RIPA lysis buffer (Pierce, Thermo Scientific, France) with protease inhibitor cocktail (1/100) and phosphatase inhibitor cocktail (1/25) (Sigma-Aldrich, France), then sonicated and centrifuged for 10 min at 12,000 g, 4 °C. Supernatants were collected and total protein concentration of each sample was determined with a BCA protein assay. Proteins were diluted in 1/1 volume with Laemmli buffer and denatured by 5 min boiling. Equal amounts (60 µg) of the denatured proteins were loaded onto a 10% SDS-PAGE gel and transferred to a PVDF nitrocellulose membrane. Membranes were cut in two at 60 kDa and blocked with PBS containing 5% bovine serum albumin (BSA) for 1 h, followed by an overnight incubation at 4 °C with the following primary antibodies: rabbit anti-P-Akt (1/1000, Cell Signaling), mouse anti-Akt (1/1000, Cell Signaling), rabbit anti-P-

FKHR (1/1000, AbCAM), rabbit anti-Fas ligand (1/1000, AbCAM) and mouse anti- $\beta$ -actin (1/5000, Sigma). Membranes were then washed 3 times and incubated 2 h with either anti-rabbit or anti-mouse horseradish peroxidase-conjugated secondary antibodies (1/2000; DAKO). Revelation was performed using the SuperSignal West-Pico Chemiluminescent Substrate (Pierce, Thermo Scientific, France). Autoradiographic films were scanned and band intensities from the generated digital images were quantified using gel tool Image J® (NIH, Bethesda, MD, USA). Akt and actin levels were used for normalization.

#### *Retrograde labeling*

Fluorogold® (Invitrogen) retrograde tracer was injected 7 days before animal sacrifice as described previously (Darlot et al., 2012; Vinit et al., 2011). Briefly, FG-C2-SCI 7 dpi rats received concomitantly a C2 hemisection and a C2 Fluorogold ipsilateral injection (just caudally to the injury); FG-C2-SCI 30 dpi rats group received the C2 FG injection (caudally to the injury scar) 23 days post SCI and were sacrificed 7 days later. FG-C4-SCI rats received concomitantly a C2 partial hemisection and a C4 Fluorogold ipsilateral injection; FG-C4-uninjured rats group (sham) received a C4 Fluorogold ipsilateral injection. Injections were performed using a 33-gauge internal cannula (C-315 I, Plastics One, Roanoke, VA, USA) connected to a 10  $\mu$ l Hamilton syringe. The cannula was inserted perpendicular to the spinal cord rostrocaudal axis, 1 mm laterally to the left from the midline with a depth of 1.8 mm from the surface of the spinal cord. After the injection of 0.75  $\mu$ l each, the spinal cord was flushed with saline solution. For analysis of respiratory neuron survival, FG retrogradely labeled cell body neurons in the VRG (0.5 to +1.8 mm rostral to the obex) were counted on approximately 5–10 transversal sections per rat respectively. No antibody amplification was used for FG detection.

#### *Immunohistochemistry and histochemistry*

Rats were sacrificed under deep anesthesia with pentobarbital (100 mg/kg, Ceva, i.p.), perfused transcardially with 300 ml of 0.1 M ice-cold phosphate buffer (pH = 7.4) followed by the same volume of 4% phosphate-buffered paraformaldehyde (pH = 7.4). Tissues were immediately dissected, post-fixed for 2 h at 4 °C in the same fixative buffer and cryoprotected 24 h at 4 °C in 30% sucrose. Tissues were then snap-frozen at –40 °C for 30 s in isopentane solution and stored at –80 °C until further use. Tissues were cut coronally into 30  $\mu$ m thick sections using a cryostat (Leica, Germany). Sections were mounted on glass microscope slides coated with 0.05% poly-L-lysine. Injury was verified by cresyl violet staining. Briefly, sections were rinsed in distilled water for 5 min and incubated 3 min in a cresyl violet bath. They were then dehydrated through a sequence of ethanol baths (70%, 95%, and 100%). Sections were finally cleaned in Xylene for 2 min and medium mounted with coverslip using Permount® (Fisher Scientific, Fair Lawn, NJ). For immunohistochemistry, medulla sections were permeabilized with PBS containing 0.2% Triton X-100 (PBS-T), immunoblocked in PBS-T with 10% normal donkey serum (NDS) for 45 min, and incubated overnight at 4 °C in the same solution with a rabbit anti-P-FKHR (1/500, AbCAM). Sections were then washed with PBS and incubated for 2 h with an Alexa Fluor® goat anti-rabbit secondary antibody (1/400, Invitrogen). After a last wash in PBS, slides were rinsed in distilled water and medium mounted with Mowiol® (Calbiochem). Cresyl violet sections were imaged using a microscope Nikon eclipse E800 and the software Axiovision. Fluorescent images were captured with an Axiovert microscope equipped with an ApoTome slider module (Zeiss) and with a 40 $\times$  lens.

#### *Intracerebroventricular treatment*

Immediately after the spinal cord surgery, rats still placed in a stereotaxic frame (Model 963; David Kopf Instrument, Tujunga, CA)

were submitted to a cannula (9 mm) implantation by stereotaxy. The skull surface was exposed by cutting the skin, cleaning and drying the skull with 10% hydrogen peroxide to highlight bone sutures. The cannula was attached to an osmotic pump via a short length of tubing and was slowly lowered into the 4th ventricle (anteroposterior: –3.6 mm from interaural line; lateral: midline; dorsoventral: +1.9 mm from interaural) and fixed in place with dental cement. A small subcutaneous pocket was then opened up on the back of the animal to fit the minipump in. Osmotic pumps (ALZET® Model 2002) were primed and filled either with a vehicle or an inhibitor of PI3K, LY294002 (2-(4-morpholinyl)-8-phenyl-4H-1-benzopyran-4-one, Promega, France) solution. LY294002 was diluted in dimethyl sulfoxide (DMSO) and administered for 21 days in the 4th ventricle at a final concentration of 5 mM in the vehicle solution containing phosphate-buffered saline (PBS, pH 7.4) with 5% DMSO. Such a concentration has been successfully used for blocking Akt activation in the brain (Bruel-Jungerman et al., 2009).

#### *Diaphragmatic electromyography*

Vehicle- and LY294002-infused rats were anesthetized using a mixture of ketamine (80 mg/kg, Imalgène 1000, Virbac, i.p.) and xylazine (20 mg/kg, Bayer, i.p.), placed in dorsal decubitus and a laparotomy was carried out. The liver was gently separated to expose the diaphragm muscle, allowing electromyography (EMG) of the diaphragm at the time-lapse of 2, 7, 14 and 21 dpi for each animal. In order to avoid scar formation due to multiple recording over time, we found that protecting the liver with humid and sterile gauze pads throughout the experiment significantly reduced the formation of scar tissue in subsequent experiments. The body temperature of the animal was maintained at 37 °C with a thermostated cover. Both right (uninjured side) and left (injured side) hemidiaphragm activities were recorded in five different areas (antero-costal, lateral, medial, postero-costal and lumbar parts), as previously described (Gauthier et al., 2006; Polentes et al., 2004). EMG diaphragm activity was recorded in several conditions: 1) during spontaneous breathing, 2) during acute hypercapnia induced by nasal occlusion performed by closing the nose of the animal during five successive breathes and 3) during an imposed progressive hypercapnic condition by adapting a 15 cm tube to the nose of the animal in order to increase the respiratory dead space and cause an hypercapnia reaching ~7% CO<sub>2</sub>. End tidal CO<sub>2</sub> was monitored using a check mate 9900 (PBI Dansensor) and ranged from 4.8% to 5.2% in eupnea to 7–7.5% during imposed asphyxic conditions in spontaneously breathing animals. Electrophysiological signals were displayed and analyzed using the LabChart software (ADInstruments). The Root Mean Square (RMS) of EMG was calculated to obtain the integrated respiratory bursts values. A bipolar electrode with a wide 2 mm inter-electrode distance has been chosen in order to prevent a very specific focal recording and allow recording of a muscular zone wide enough to cover a large part of each specific diaphragm area cited above. Such electrode specificity allowed the management of a reliable recording of diaphragm across time. To ensure valid comparison between left and right hemidiaphragm activities and also between different rats across time, the same bipolar electrode was used for the left and right hemidiaphragm recordings of similar muscular sites. Between two paired (left and right) hemidiaphragm area recordings, we verified the stability of the ventilator status of the animal by recording back the first diaphragm area and checking that the amplitude of the EMG signal was analogous to the one previously recorded. The total time procedure for each animal was limited to 1 h. EMG quantitations during eupnea and progressive hypercapnia were performed by analyzing 10 of a total of ~18 to 20 successive respiratory bursts occurring during a stable bursting period of around 20 s. During progressive hypercapnia, the respiratory frequency increases during the first 15–20 s after the onset and then remains stable. It is only after this latency period that the 10 respiratory bursts were analyzed (i.e. around 30–60 s after the onset of the procedure). During acute asphyxia induced by

nasal occlusion, an increase of respiratory burst was observed from the first EMG burst. For ethical reasons the nasal occlusion was maintained only for 8 s, during which ~6–8 bursts occurred. EMG quantitation was performed by analyzing the first 5 bursts. The average of these values from vehicle and LY294002-infused conditions was calculated from the medial areas and used to represent 1) the percentage of change from baseline eupnea in order to report the responses to respiratory challenges ( $100 \times (\text{hypercapnia value} - \text{eupnea value}) / \text{eupnea value}$ ) and 2) the ratio of left versus right hemidiaphragm ( $100 \times \text{left value} / \text{right value}$ ).

#### Images analyses

Quantitation of P-FKHR pixels within the medulla was performed by outlining areas measuring 1,443,520 pixels and splitting RGB channels. Images were converted to 8 bit type images, binary processed and a similar threshold was applied to normalize staining between sections. Limit to threshold was checked to include in measurement calculations only thresholded pixels. Numbers of P-FKHR positive pixels were then counted using the measure tool of Image J software.

#### Statistical analysis

All results are presented as mean  $\pm$  SEM. Statistical analyses were performed using Prism version 4.0 (GraphPad Software, CA). Immunoblot and immunohistochemistry data were analyzed using two tailed Mann–Whitney test or one-way ANOVA followed by Bonferroni post-test. Changes in diaphragm recovery over time (2, 7, 17, 21 dpi) from same rats were analyzed using the repeated measure one-way ANOVA test. Comparison of vehicle and LY294002 treatment over time was analyzed using the repeated measure two-way ANOVA. Differences were considered significant if  $p < 0.05$ .

## Results

### *Partial cervical SCI induces FKHR inactivation and increases Akt phosphorylation in the medulla oblongata*

We performed an incomplete hemisection at the C2 spinal cord level which interrupts both descending motor and lateral ascending sensory tracts within the lateral funiculi of the spinal cord (Anderson et al., 2005; Vinit et al., 2006). This injury model severs descending bulbospinal tracts including the inspiratory drive originating from the medulla oblongata of the brainstem and projecting to phrenic motoneurons (Krassioukov, 2009) (Fig. 1).

We first hypothesized that if post-lesion molecular changes occur in cell bodies of injured neurons located within the medulla in response to SCI, then this would probably arise from a specific genetic program that may be orchestrated by the activation or inactivation of specific transcription factors (Fig. 1). It is well known that processes such as cell growth, neuroprotection and inflammation appear during the first months after spinal cord injury. We thus investigated such molecular events using a DNA–protein array-based screening assay that profiles simultaneously the activity of 20 transcription factors involved in such cellular processes (Figs. 2A, B). We prepared protein nuclear extracts from medulla slices encompassing the rostral ventral respiratory group (VRG), and the raphe pallidus of uninjured (sham) and injured (SCI) rats (7 days post-injury (dpi) and 90 dpi) in order to perform a differential screening on areas involved in respiratory function. Quantitation and comparison of spot intensities of the arrays between conditions (SCI versus uninjured) revealed that activities of many transcription factors (AP1, c-Myb, CREB, E2F-1, EGR,...) were unchanged at 7 or 90 dpi in comparison to uninjured condition (Figs. 2C, D). Spots for OCT-1 were undetectable for all conditions (uninjured and injured) and for both concentration (neat or 1/10 diluted) suggesting that this transcription factor might be inactive, or even unexpressed, in the brain

region considered here. At 7 dpi (Fig. 2C), of the 20 analyzed transcription factors, 4 of them were identified on the basis of an activity considered significantly different from uninjured condition (more than 2-fold) (FKHR, Myc-Max, PPAR $\gamma$  and SRE). At 90 dpi (Fig. 2D), using the same criteria of significance, only 1 factor, FKHR (Forkhead transcription factor, FOXO1A), was identified. Thus, FKHR was the only factor observed to vary significantly at the two time points after SCI. Indeed, compared to uninjured condition, FKHR activity was undetectable at 7 dpi and down-regulated by  $76 \pm 2\%$  at 90 dpi.

Since FKHR inactivation requires Akt phosphorylation (Brunet et al., 1999), we next assessed Akt phosphorylation status by immunoblotting total protein extracts from brain slices encompassing the same medulla regions as described above (Fig. 3). Proteins were obtained from uninjured (sham) and 2, 7 and 15 dpi (SCI) rat groups. Quantitation of the P-Akt/Akt ratio revealed a 3-fold increase of P-Akt in the medulla of SCI rats compared to the medulla of uninjured ones ( $p < 0.05$  at 2 and 15 dpi;  $p < 0.01$  at 7 dpi, one-way ANOVA followed by Bonferroni post test).

These results show that the PI3K/Akt signaling pathway is activated in the medulla after SCI, resulting in the inactivation of the apoptosis-inducing factor, FKHR, one of the P-Akt downstream targets. Thus, considering the known function from the literature of this cell-signaling pathway in survival and plasticity, we decided to further investigate its role.

### *Partial cervical SCI upregulates P-FKHR in respiratory premotoneurons*

In order to directly assess whether cell bodies of bulbospinal tract neurons involved in the respiratory function might respond to SCI, we combined P-FKHR immunohistochemistry with Fluorogold (FG) retrolabeling of bulbospinal neurons.

To compare this response to basal levels of P-FKHR in uninjured condition, we used a group of rats that were uninjured (sham) but received a FG injection at the C4–C5 ventral horn level, where respiratory bulbospinal tract contact phrenic motoneurons pool. In medulla slices of these uninjured FG-C4 rats, retrogradely labeled-FG positive cell bodies were detected in VRG and raphe pallidus structures 7 days after FG injection (Figs. 4A and B). A weak cytoplasmic P-FKHR immunoreactivity was detected in both VRG and raphe pallidus retrolabeled-FG neurons (Figs. 4A and B). We then compared uninjured FG-C4 rats with SCI rats receiving a C2 ipsilateral FG injection restricted to the injury site. In these FG-SCI animals, FG was mainly captured by axotomized neurons of the bulbospinal tract (Darlot et al., 2012; Vinit et al., 2005, 2011). In contrast to the sham condition (FG-C4), both VRG and raphe pallidus FG injured neurons displayed a significantly higher level of cytoplasmic P-FKHR immunoreactivity (Figs. 4C, D, G and H) ( $p < 0.01$  for VRG and raphe pallidus, one-way ANOVA followed by Bonferroni post test).

Since the activation of P-FKHR in response to neuronal injury may not be limited to axotomized neurons, we investigated its expression in C2-injured rats that received FG injection in the C4–C5 ventral horn in order to label respiratory neurons with spared axons projecting beneath the injury (Figs. 4E and F). In these FG-C4-SCI animals, FG diffusion in the spinal cord was restricted to the ipsilateral side and did not reach the site of the injury (Darlot et al., 2012). Thus, using this setting, FG is principally captured by non-axotomized terminals traveling into the medial part of the spinal cord and occasionally by contralateral axons that may cross the spinal midline at the C4–C5 levels, as reported previously (Boulenguez et al., 2007). In the medulla of these FG-C4-SCI rats, FG positive neurons were observed in the same areas as uninjured FG-C4 and FG-C2-SCI rats, but as previously found for the VRG (Darlot et al., 2012), they were less numerous than in FG-C4 rats (Figs. 4A, C and E). However, as was the case for axotomized FG neurons (Figs. 4C and D), both VRG and raphe pallidus FG spared neurons displayed significantly higher level of cytoplasmic P-FKHR immunoreactivity

## Does the Medulla Oblongata contribute to the spontaneous respiratory recovery after SCI ?

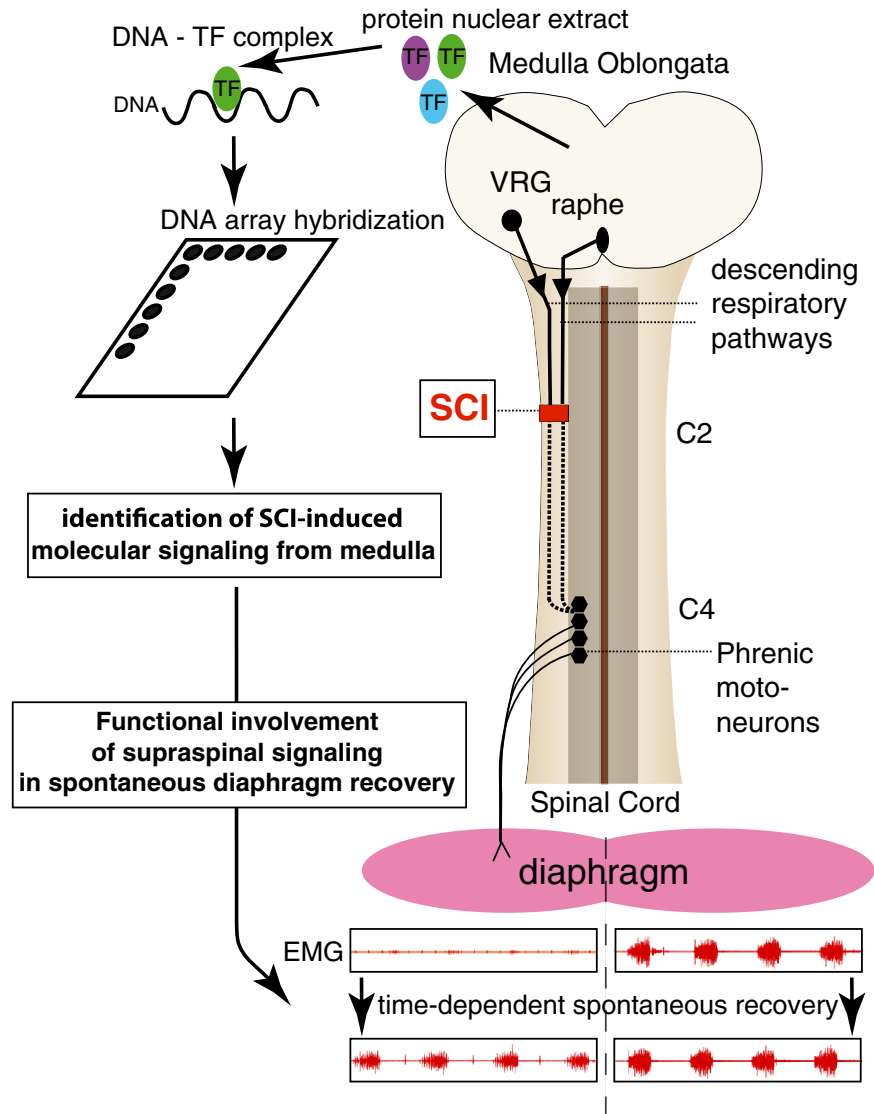


**Fig. 1.** Schematic illustration of the working hypothesis and experimental paradigm. We hypothesized that SCI may induce a supraspinal cell-signaling which could contribute to the functional respiratory recovery. This hypothesis was addressed using a lateral incomplete hemisection of the cervical (C2 level) spinal cord, a model of mild injury known to sever descending fibers including those of premotoneurons of the respiratory system originating from the VRG and raphe and connecting to the phrenic motoneuron pool. Such cervical injury is sufficient first to abolish the ipsilateral hemidiaphragm contractility and then to induce a time-dependent recovery of this hemidiaphragm. In order to identify supraspinal cell-signaling pathways, we collected medulla oblongata tissues and screened for activity of transcription factors using DNA/protein array (see [Material and methods](#) section). Using pharmacological inhibition, we addressed the functional contribution of the medulla oblongata in the recovery of the respiratory system. TF: transcription factor; VRG: ventral respiratory group; C2, C4: cervical spinal cord metamer level.

compared to the uninjured condition (Figs. 4E–H) ( $p < 0.05$  for VRG and raphe pallidus, one-way ANOVA followed by Bonferroni post test).

In the medulla, an increase of the P-FKHR immunoreactivity was also observed beyond the VRG and raphe areas. Since the extent of injury we performed not only restricts to the respiratory pre-motoneurons but also damages other pre-motoneurons, it is possible that P-FKHR activation might be a ubiquitous neuronal response after injury.

To assess whether such P-FKHR activation might be correlated with neuroprotection of axotomized respiratory-related neurons, we counted and compared the number of retrogradely labeled VRG neurons between sham uninjured (FG-C4) and injured rats (FG-C2; 7 dpi and 30 dpi). The number of FG positive cell bodies appeared quite similar in these two animal groups (Fig. 4I).

Collectively, these results suggest that these respiratory-related neurons inactivate the pro-apoptotic downstream target of PI3K/Akt: FKHR, and thus survive after injury to their axon.

*Delivery of the PI3K inhibitor, LY294002, decreases injury-induced phosphorylation of Akt and FKHR and activates Fas ligand in the medulla oblongata*

We next tested whether this cell-signaling activation might be blocked through in vivo pharmacological treatment using the drug LY294002, an inhibitor of PI3K (Vlahos et al., 1994). In order to get access to the medulla oblongata, SCI rats received 4th ventricular infusion of either LY294002 or vehicle solution via osmotic minipumps

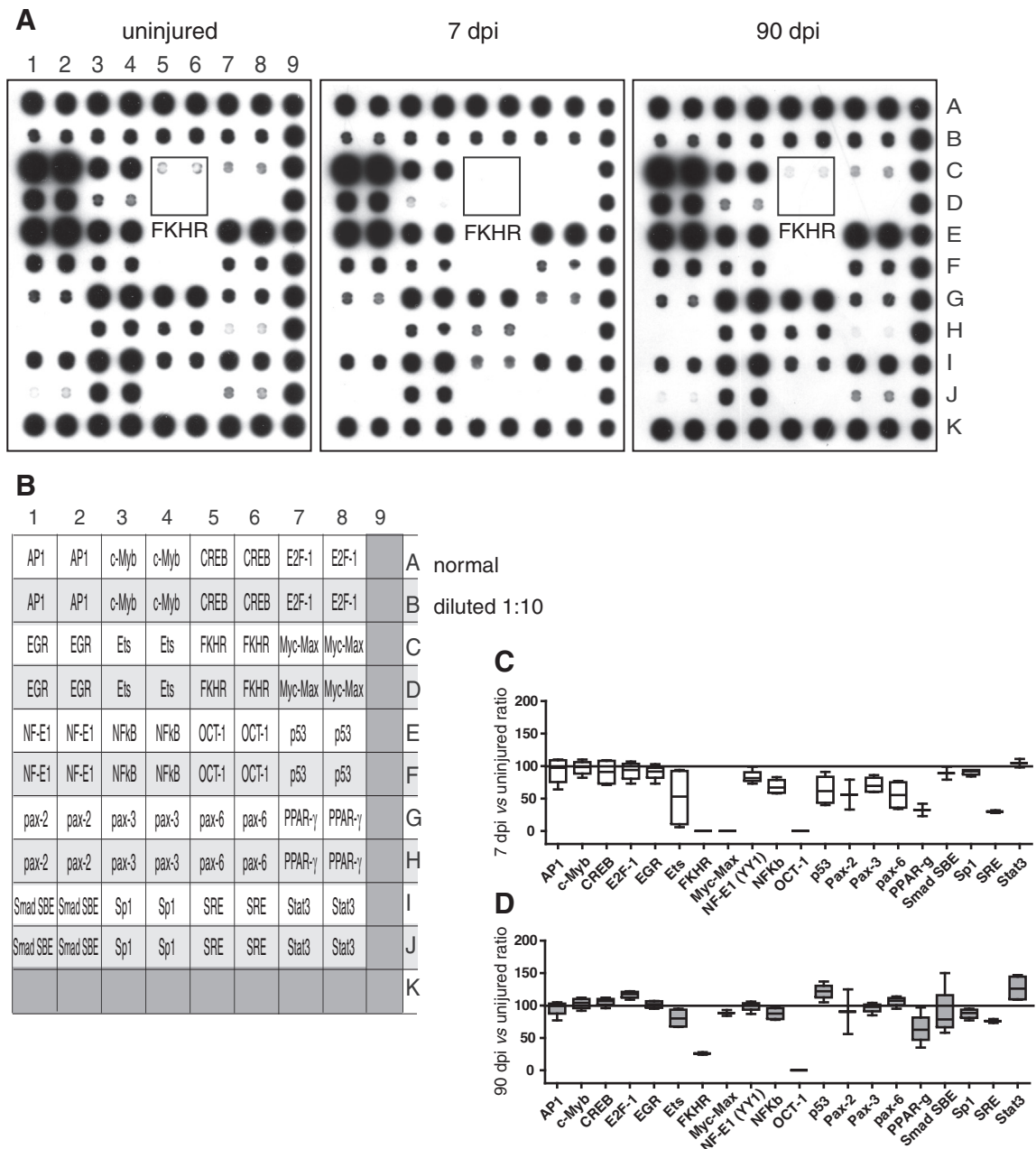


**Fig. 2.** Inactivation of FKHR and phosphorylation of P-Akt after partial cervical SCI. (A) DNA/protein array analysis of medulla activated transcription factors in uninjured and SCI (7 and 90 dpi) rats. Each transcription factor oligonucleotide recognition sequence is spotted on the membrane neat and diluted 1:10 providing a dynamic range of signal intensity. (B) Transcription factor labels: AP-1: Activator Protein 1; c-Myb; CREB: cAMP Response Element Binding protein; E2F-1: E2F transcription factor 1; EGR: Element Growth Response; Ets: Erythroid transcription; FKHR: Forkhead in Rhabdomyosarcoma; Myc/Max; NF-E1 (YY1): Nuclear Factor Erythroid-derived 1 (YY1 transcription factor); NFKB: Nuclear Factor-kappa B; OCT-1: Octamer binding transcription factor 1; P53: protein 53; Pax-2: paired box gene 2; Pax-3: paired box gene 3; Pax-6: paired box gene 6; PPAR- $\gamma$ : Peroxisome Proliferator-Activated Receptor  $\gamma$ ; Smad/SBE: Smad/Smad-Binding protein; Sp1: Specificity Protein 1; SRE: Serum Response Element; Stat3: Signal transducer and activator of transcription. (C and D) Transcription factor activity ratio between 7 dpi (SCI) versus uninjured (sham) animals (C) and 90 dpi versus uninjured animals (D). An arbitrary 2-fold change cutoff was established for significance. dpi: days post-injury.

(Fig. 5). LY294002 and vehicle solutions were infused for 21 days starting the day of the SCI (Fig. 5A). Body weight was measured daily during the treatment period in order to ensure that LY294002 infusion did not affect the general health of the animals and also because breathing activity is animal weight-dependent (Fuller et al., 2008) (Fig. 5B). For both vehicle and LY294002-infused rats, SCI produced a similar initial weight loss with a maximum at 4–5 dpi. For both conditions, body weights returned to pre-surgical level by 10 dpi after which it increased for the two animal groups. Thus, since LY294002 treatment has no effect

on body weight, vehicle-infused rats could be used as a weight-matched group for breathing comparison with LY294002-infused ones.

Medulla slices of SCI rats encompassing VRG and raphe pallidus areas were collected 21 days after 4th ventricular infusion to assess the biochemical consequences of LY294002 action (Fig. 5C). Western blots analyses revealed that SCI-induced phosphorylation of Akt was significantly decreased by almost 2-fold in LY294002-infused rats compared to vehicle ones ( $p < 0.05$ , Mann-Whitney). Similarly, a decrease in phosphorylation was observed for the downstream target of Akt:

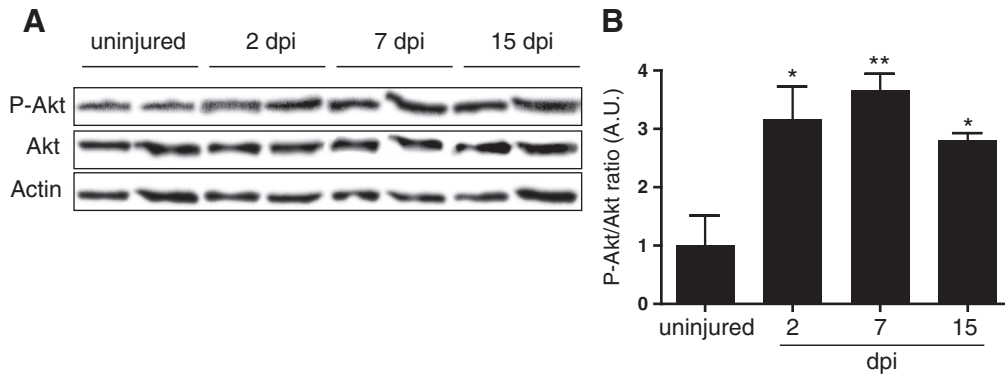


**Fig. 3.** P-Akt activation in the medulla oblongata after partial cervical SCI. (A) Immunoblots of medulla P-Akt, Akt and actin expression in uninjured and SCI rats at 2, 7, 15 dpi. At all-time points, injury produces an increase of P-Akt content in the medulla oblongata of the brainstem. (B) Quantitation of P-Akt content in medulla oblongata. P-Akt content was normalized to protein content of Akt. \*:  $p < 0.05$  and \*\*:  $p < 0.01$ , Bonferroni post hoc. dpi: days post-injury.

FKHR ( $p < 0.05$ , Mann–Whitney). Furthermore, the protein level of Fas-ligand, one of the FKHR downstream targets, was significantly increased by 2-fold in LY294002-infused rats compared to vehicle treated animals ( $p < 0.01$ , Mann–Whitney).

Thus, these results validate the efficiency of LY294002 treatment in reducing SCI-induced PI3K/Akt signaling pathway within the medulla. Finally, we examined the protein level of P-Akt at the cervical spinal cord level in the two animal groups. Western blot analyses revealed that the phosphorylation level of P-Akt was similar in LY294002-infused rats compared to vehicle ones (Fig. 5D). Thus, during this period of treatment, the inhibitory action of the LY294002 drug did not extend to the cervical spinal cord level but was restricted to the brain.

#### *Inhibition of medulla P-Akt reduces the spontaneous respiratory recovery observed after cervical incomplete hemisection*

To gain insight into the functional contribution of this signaling pathway, we evaluated the potential of the LY294002 drug to prevent the spontaneous respiratory recovery of injured rats during the 21 days of 4th ventricular infusion. Respiratory-related diaphragm activity of injured rats was recorded at 2, 7, 15, 21 dpi allowing matched repeated measures for each condition (LY294002 and vehicle-infused rats) (Fig. 6).

Fig. 6 represents examples of EMG activity of left (ipsilateral injured-side) and right hemidiaphragms (contralateral uninjured-side) recorded from the vehicle (Fig. 6A) and LY294002 injured rats (Fig. 6B). In both conditions, ipsilateral hemidiaphragm EMG bursts were unitary or absent at 2 and 7 dpi, while as expected, contralateral hemidiaphragm presented massive EMG bursting. By 15 dpi, a robust EMG signal could be recorded from the ipsilateral hemidiaphragm of the vehicle-infused rats (Fig. 6A). However, at the same post-injury stage, EMG activity of the ipsilateral hemidiaphragm remained unitary or absent in the LY294002-infused rats (Fig. 6B). Finally by 21 dpi, EMG bursts of the vehicle-infused rats were similar between the ipsilateral and contralateral hemidiaphragms (Fig. 6A). In contrast, such full recovery was not observed at 21 dpi for the LY294002 condition where EMG activity of ipsilateral hemidiaphragm remained unitary, with a weak activity always less robust than that of the contralateral hemidiaphragm (Fig. 6B). LY294002 had no side effect on the respiratory activity since both contralateral (non-paralyzed) hemidiaphragms of vehicle and LY294002-infused rats behave similarly in terms of contractility over time.

Quantitation of integrated EMG bursts over time of recovery revealed that ipsilateral diaphragmatic EMG of vehicle-infused rats increased in a time-dependent fashion ( $p < 0.0001$ , repeated measure one-way ANOVA), differing significantly from LY294002-infused rats

( $p < 0.05$ , repeated measure two-way ANOVA) (Fig. 6C). Differences in integrated EMG bursts between vehicle and LY294002-infused rats became significant at 15 and 21 dpi (Fig. 6C;  $p < 0.05$  and  $0.01$  respectively, Mann–Whitney test). In contrast to vehicle-infused rats, ipsilateral diaphragmatic EMG bursts of LY294002-infused rats did not significantly differ over time but remained weak (Fig. 6C). Collectively, these results show that while the ipsilateral hemidiaphragm of vehicle-infused rats spontaneously recovers by 21 dpi, medullary inhibition of the PI3K/Akt signaling pathway prevents similar recovery. However, respiratory frequency remained similar between vehicle and LY294002 conditions and stable over time (Fig. 6D).

#### *Inhibition of medulla P-Akt does not alter the ventilatory response to respiratory challenge after cervical incomplete hemisection*

In addition to these electrophysiological experiments in eupneic conditions, we also evaluated whether brainstem infusion of LY294002 could alter the sensitivity or the amplitude of the hypercapnic chemoreflex response (Fig. 7). Diaphragm contractile frequency and contractile force were thus respectively recorded during progressive hypercapnic (Fig. 7A1) and acute asphyxia (Fig. 7A2) conditions. Results were obtained from longitudinal experiments in SCI rats at 2, 7, 15, 21 dpi, allowing matched repeated measures within conditions (LY294002 and vehicle-infused rats) (Figs. 7 B–E).

For both vehicle and LY294002 conditions, progressive hypercapnia increased respiratory frequency by more than 50% from eupnea baseline (Fig. 7B). For all-time points examined, comparison of frequency responses between vehicle and LY294002-infused rats revealed similar percentage of increase during progressive hypercapnia, with stable changes over the 21 days period.

During acute asphyxia, quantitation of integrated EMG over time of recovery revealed that diaphragm contractility (ratio of left versus right hemidiaphragms) of vehicle- and LY294002-infused rats increased as a function of time after SCI (Fig. 7C;  $p < 0.001$  for both conditions, repeated measure one-way ANOVA). However, diaphragm contractility of vehicle-infused rats was significantly higher than LY294002-infused rats (Fig. 7C;  $p < 0.05$ , repeated measure two-way ANOVA). Differences in integrated EMG bursts between vehicle and treated conditions became significant at 15 and 21 dpi (Fig. 7C;  $p < 0.05$ , Mann–Whitney test). Despite this difference between the vehicle and LY294002 rat groups, the left and right diaphragms of both groups responded to acute asphyxia by increasing their contractile force by more than twice from eupnea baseline (Figs. 7D and E). Comparison of contractile force responses to acute asphyxia between vehicle and LY294002-infused rats revealed similar percentage increase with stable changes over the 21 days period (Figs. 7D and E).

Collectively these results demonstrate that LY294002 treatment does not affect the capacity of the respiratory system to respond to hypercapnic challenges by increasing the respiratory frequency and the diaphragm contractility. However, while LY29

4002-infused rats retained a capacity to compensate by hyper-ventilation similarly to vehicle-infused rats, the contractile force of their diaphragm was significantly lower than vehicle-infused animals.

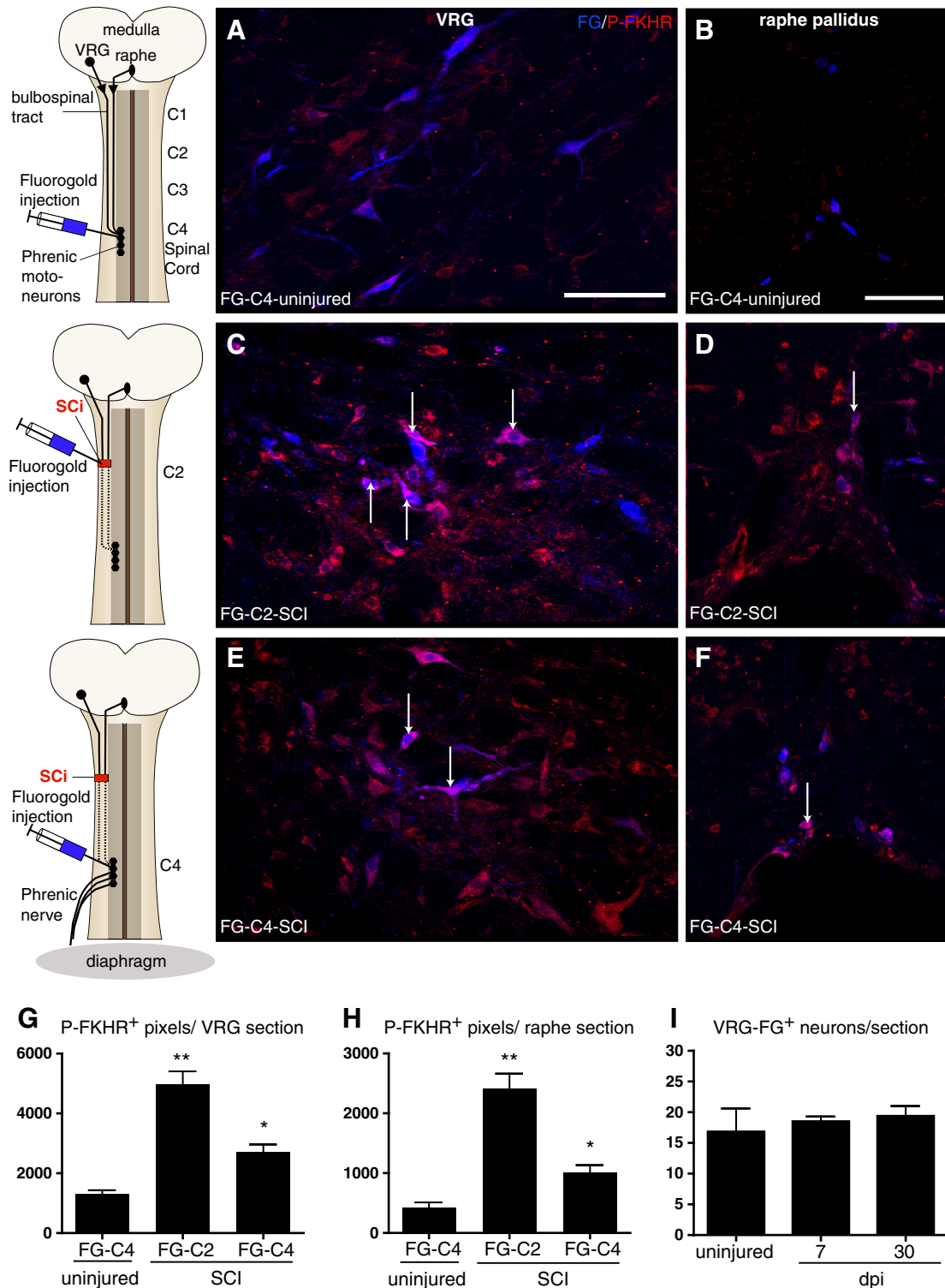


**Fig. 4.** P-FKHR immunoreactivity in cell bodies of injured Fluorogold retro-labeled axons. Description insets illustrating the Fluorogold (FG) injection sites performed in three different rat groups: FG-C4-uninjured; FG-C2-SCI and FG-C4-SCI. (A, C, E) Immunohistochemistry for P-FKHR (red) and revelation of Fluorogold retrograde tracer (blue) in VRG of FG-C4-uninjured (A), FG-C2-SCI (C) and FG-C4-SCI (E) rats. (B, D, F) Immunohistochemistry for P-FKHR (red) and revelation of Fluorogold (blue) in raphe pallidus of FG-C4-uninjured (B), FG-C2-SCI (D) and FG-C4-SCI (F) rats. Scale bar: 100  $\mu$ m. Arrowheads point out P-FKHR and FG co-labeled cells. (G–H) Quantitation of P-FKHR immunoreactivity in the VRG and raphe pallidus, respectively. \*:  $p < 0.05$  and \*\*:  $p < 0.01$ , Bonferroni post hoc. Note that P-FKHR immunoreactivity is more intense in neurons of SCI rats than uninjured rats, whether they are axotomized neurons (FG-labeled in FG-C2-SCI rats) or spared neurons (FG-labeled in FG-C4-SCI rats) (I) Quantitation of the number of VRG Fluorogold retro-labeled neurons in uninjured and injured (7 dpi and 30 dpi rats) conditions.

**Discussion**

In this study, we hypothesized that supraspinal structures may contribute to post-lesional spontaneous recovery after SCI. At the molecular level, such hypothesis presumes that cell-signaling pathways might be

activated in supraspinal areas in response to SCI. We addressed this hypothesis using a cervical (C2) incomplete hemisection that axotomized the ipsilateral bulbospinal respiratory tract which originates from respiratory neurons of the medulla oblongata and controls the phrenic motoneurons. This SCI model allows a time-dependent spontaneous

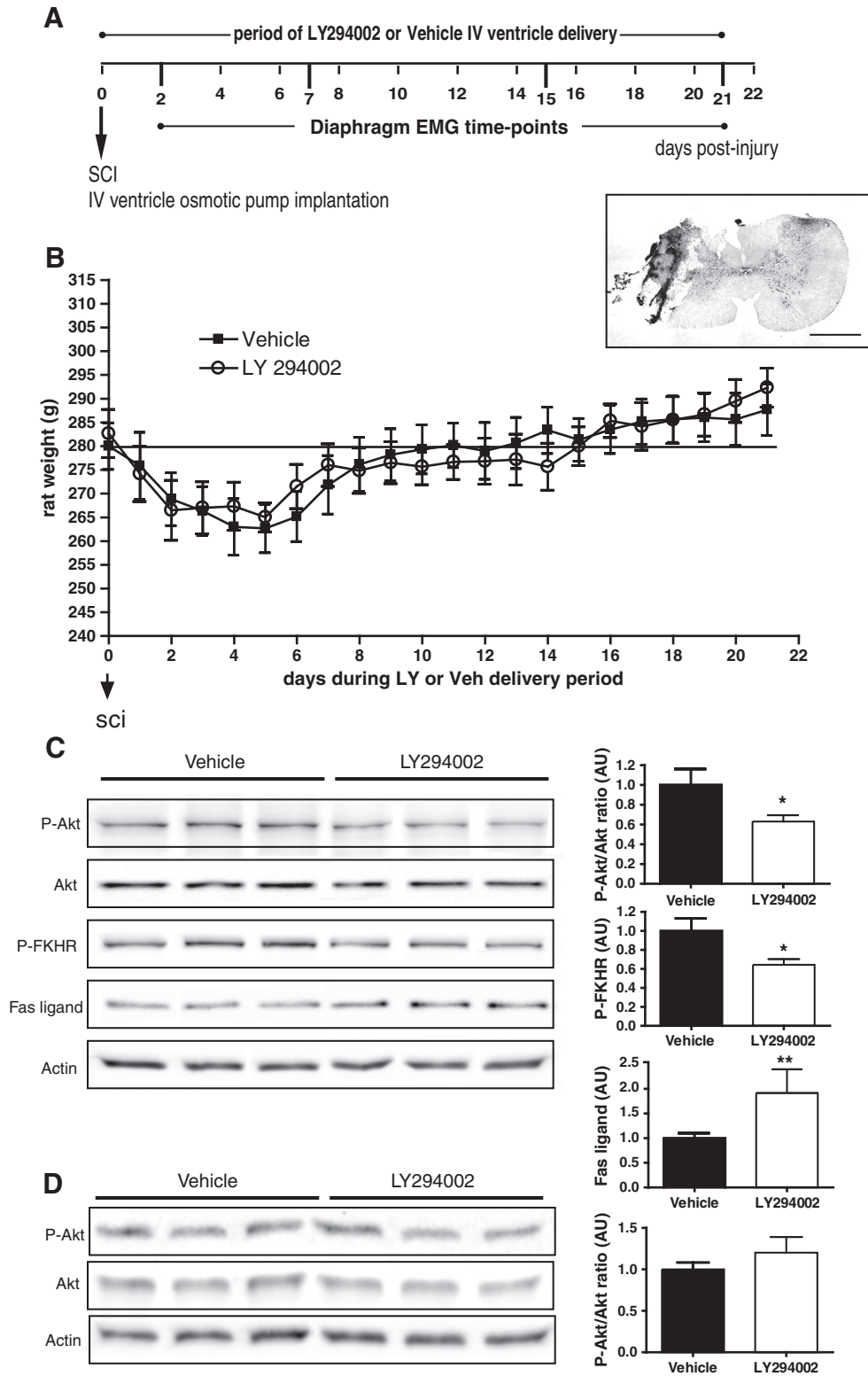


**Fig. 5.** Experimental paradigm of LY294002 4th ventricular delivery and validation of medulla P-Akt inhibition. (A) Experimental paradigm. Animals were submitted to SCI and osmotic pump implantation. Control animals were injected with a vehicle solution whereas treated ones received the PI3K inhibitor solution. Diaphragm EMG recordings were performed at 2, 7, 15 and 21 days post-injury. Cresyl violet staining illustrates the SCI. Scale bar: 1 mm (B) Rat weight measurement during the 21 days of the experiment. (C) Immunoblots and quantitative analyses of P-Akt, Akt, P-FKHR, Fas-ligand expression in the medulla. (D) Immunoblots and quantitative analysis of P-Akt, Akt expression in the spinal cord at C4 level.

respiratory recovery (Goshgarian, 2003, 2009; Lane et al., 2008, 2009; Vinit and Kastner, 2009; Vinit et al., 2008). By screening for molecular candidates in the medulla oblongata using a DNA/protein array, we initially found that the activity of the forkhead transcription factor (FKHR or FOXO1A) is the most depressed after SCI. The fact that

phosphorylation of this pro-apoptotic transcription factor requires PI3K-Akt activation and that we also demonstrated an increase of Akt phosphorylation in the medulla after SCI strongly argue for the involvement of Akt in the time-dependent respiratory recovery (Fig. 8).

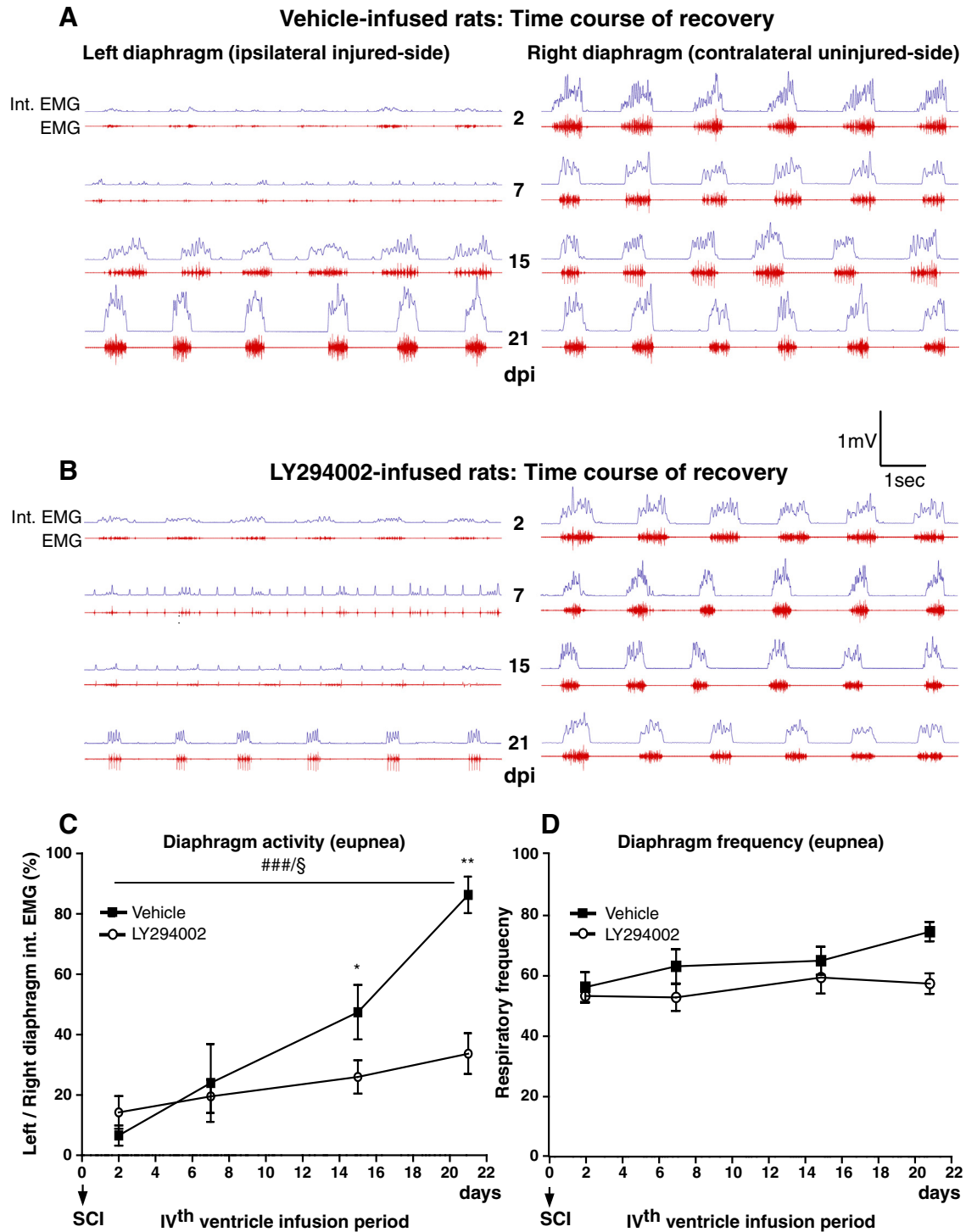
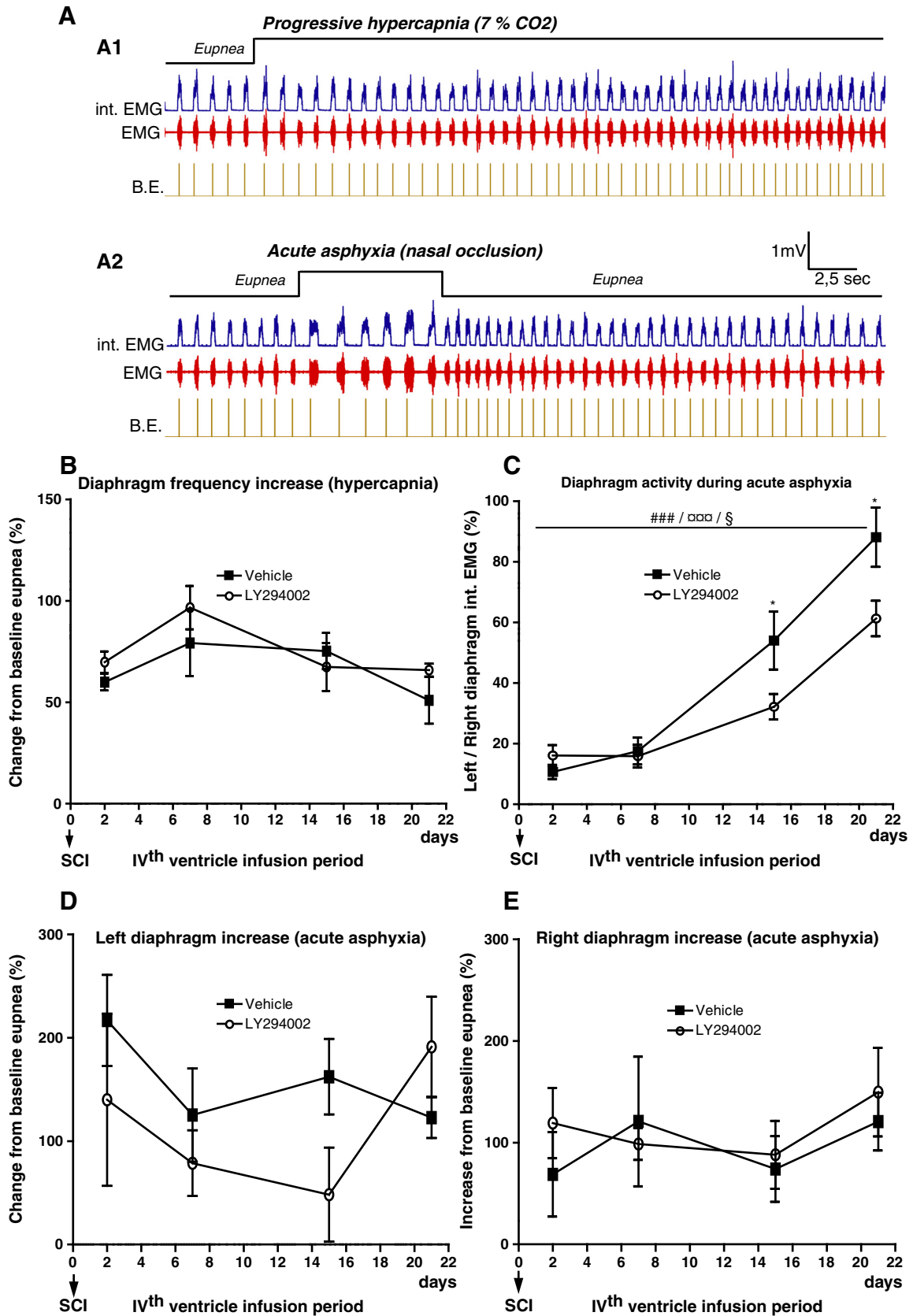


**Fig. 6.** Effect of LY294002 medulla treatment on the spontaneous time-dependent respiratory recovery after cervical incomplete hemisection. (A–B) Examples of inspiratory hemidiaphragmatic EMG bursts, raw and integrated (int.), in vehicle (A) versus LY294002-infused (B) rats, recorded at 2, 7, 15 and 21 dpi. SCI produced for both vehicle and LY294002-infused rats a comparable left hemidiaphragm paralysis. As expected, complete spontaneous recovery was observed by 21 dpi in control condition (vehicle-infused rats). Such time-dependent recovery was not observed for the treated condition (LY294002-infused rats). (C) Quantitation of diaphragm activity (expressed as the ratio of left versus right integrated EMG values) over time of recovery in vehicle and LY294002-infused rats. Recovery of the left diaphragm of vehicle-infused rats increased significantly over time (###:  $p < 0.001$ , repeated one-way ANOVA) and differed significantly from LY294002-infused rats (§:  $p < 0.05$ , repeated two-way ANOVA). Differences in integrated EMG burst ratio between conditions became significant at 15 and 21 dpi (\*:  $p < 0.05$ , \*\*:  $p < 0.01$ , Mann–Whitney test). (D) Respiratory frequency values (measured by the number of diaphragmatic bursts per minute) over time of recovery in vehicle and LY294002-infused rats.



Among the different cell-signaling pathways involved in neuronal response after injury, PI3K/Akt is positioned at the intersection of multiple signals and functions (Aberg et al., 2003; Brazil et al., 2004; Brunet

et al., 1999; Burgering and Kops, 2002; Dudek et al., 1997; Noshita et al., 2002; Yu et al., 2005; Zhao et al., 2005). The canonical PI3K/Akt signaling pathway promotes cell survival by inhibiting the activation of pro-

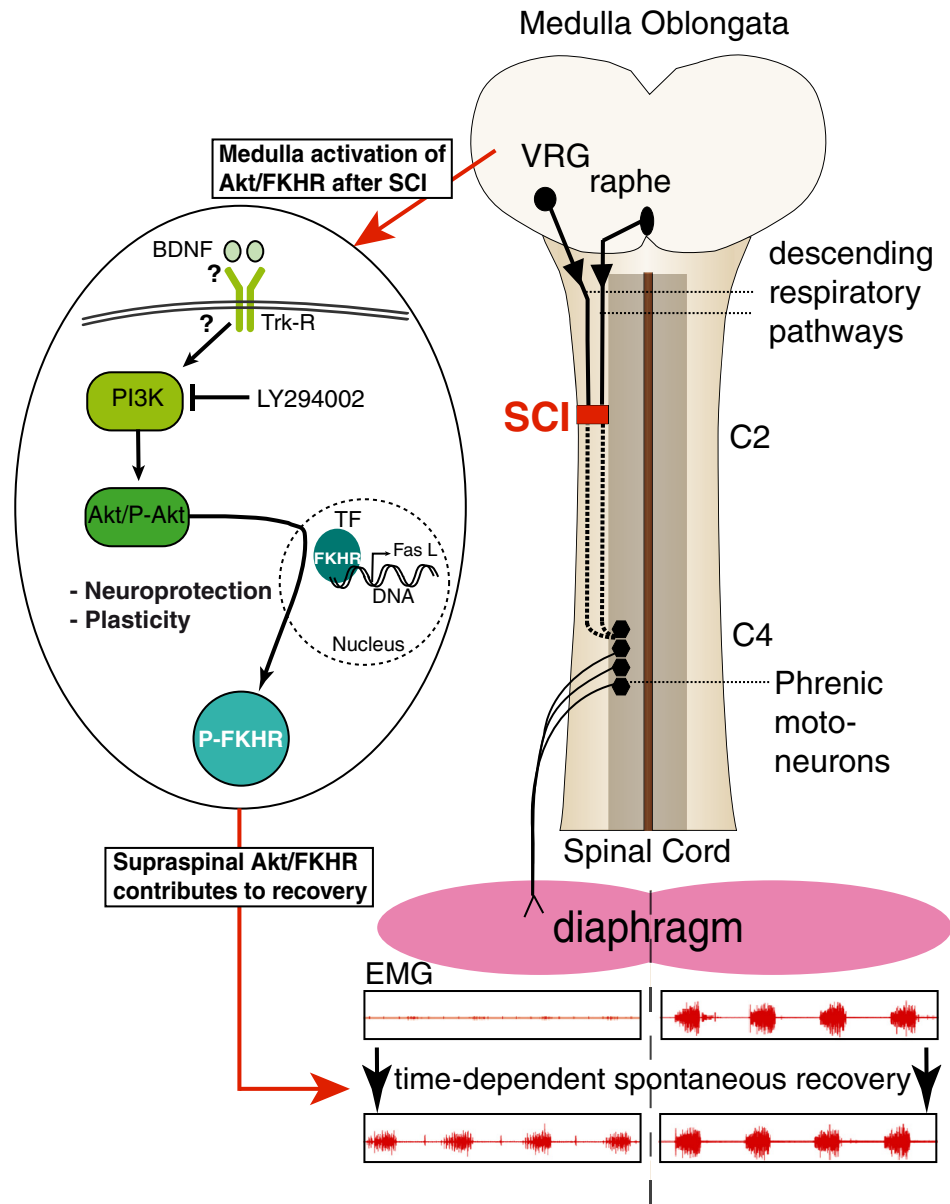


**Fig. 8.** Schematic illustration of the contribution of Akt/FKHR cell-signaling pathway to spontaneous respiratory recovery. In this study we have shown that after partial cervical hemisection (SCI), the Akt/FKHR cell-signaling pathway is activated in the medulla oblongata of the brainstem. In-vivo pharmacological blockade of this cell-signaling pathway, using the LY294002 PI3K inhibitor, prevents the diaphragmatic spontaneous recovery suggesting that supraspinal structures contribute to the time-dependent respiratory recovery. Considering the literature, it might be possible that BDNF triggers this cell-signaling. TF: transcription factor; VRG: ventral respiratory group; C2, C4: cervical spinal cord metamerical level.

apoptotic proteins, including FKHR (Brunet et al., 1999; Burgering and Kops, 2002; Dudek et al., 1997; Noshita et al., 2002; Yu et al., 2005; Zhao et al., 2005). Furthermore, the activation of Akt is implicated not only in other functions like glucose metabolism and protein synthesis but also in synaptic plasticity such as long-term potentiation in the dentate gyrus and erythropoietin-induced phrenic motor facilitation (Bruel-Jungerman et al., 2009; Dale et al., 2012; Horwood et al., 2006). Thus, considering our results and the major known roles of PI3K/Akt/

FKHR, we selected this pathway as an interesting candidate potentially involved in supraspinal neuroprotection and plasticity after injury.

We found that the cell bodies of injured respiratory-related neurons located in the medulla oblongata (ventral respiratory group and raphe pallidus neurons) express high levels of P-FKHR. As evaluated by the number of retrograde labeled respiratory-related neurons, partial SCI does not produce a massive loss of VRG injured neurons, a result that fits also with the observation of an unchanged number of respiratory

**Fig. 7** Effect of LY294002 medulla treatment on the respiratory response during hypercapnic challenge. (A) Examples of inspiratory diaphragmatic EMG bursts, raw and integrated (int.), in response to two hypercapnic challenges: progressive hypercapnia (A1) and acute asphyxia (A2). B.E.: Burst event (from inspiratory EMG). (B) Effect of progressive hypercapnia on diaphragm contractile frequency (expressed as the percentage of increase from baseline eupnea) over time in vehicle and LY294002-infused rats. Vehicle and LY294002-infused rats similarly increase their respiratory frequency in response to progressive hypercapnia. (C) Quantitation of diaphragm activity in response to acute asphyxia (expressed as the ratio of left versus right integrated EMG values) over time in vehicle and LY294002-infused rats. Response to acute asphyxia of the left diaphragm of vehicle and LY294002-infused rats increased significantly over time (###:  $p < 0.001$ , □□□:  $p < 0.001$  respectively, repeated one-way ANOVA). However, LY294002 treatment significantly reduced the contractile capacity of left hemidiaphragm (§:  $p < 0.05$ , repeated two way ANOVA). Differences in integrated EMG burst ratio between conditions became significant at 15 and 21 dpi (\*:  $p < 0.05$ ). (D–E) Quantitation of left (D) and right (E) hemidiaphragm contractility in response to acute asphyxia (expressed as the percentage of increase from baseline eupnea) over time in vehicle and LY294002-infused rats. Vehicle and LY294002-infused rats were similarly reactive to acute asphyxia.

bulbosplinal fibers at C1 level, 7 days after incomplete C2 hemisection (Darlot et al., 2012). Thus, these data highlight that partial SCI is not correlated with a loss in the number of medulla premotoneurons but with an activation of the PI3K/Akt/FKHR signaling pathway in the medulla premotoneurons including the respiratory ones. Furthermore, we showed here that *in vivo* pharmacological blocking of Akt phosphorylation led to an inhibition of FKHR phosphorylation and an increase of expression of one of its pro-apoptotic target proteins, Fas ligand. Such medullary inhibition does not affect the phosphorylation state of Akt at the spinal level. Considering the canonical action of PI3K/Akt/FKHR it is thus possible that this cell-signaling contributes to a form of innate brain neuroprotection from SCI. In support to this hypothesis, inhibition of PI3K/Akt by the LY294002 drug is known to suppress brain neuroprotection after cerebral ischemia by inhibiting phosphorylation of FKHR (Zhan et al., 2012); or to aggravate spinal secondary damages after SCI (Paterniti et al., 2011). Furthermore, the demonstration of an innate neuroprotection after injury that would restrict neuronal loss has been recently made at the spinal cord level (Sabelstrom et al., 2013). Thus after SCI, our data suggest that the activation of the Akt/FKHR signaling pathway in the medulla might be involved in innate neuroprotection and that the same cell-signaling pathway of neuroprotection might coexist at the spinal and supraspinal levels.

The main result of the present study is the demonstration that this activated supraspinal pathway contributes to the recovery of the respiratory function after SCI (Fig. 8). Indeed, we showed that medulla delivery of the PI3K inhibitor, LY294002, prevents the diaphragmatic spontaneous recovery which is normally observed by 21 dpi in the vehicle-infused rats. Considering the importance of plasticity mechanisms in this functional recovery, it can be argued that medullary activation of PI3K/Akt pathway might be involved in post-lesional plasticity rather than in aspects of neuroprotection. At least three points in favor of a post-lesional plasticity hypothesis can be considered.

Firstly, respiratory recovery after partial cervical injury has been partly attributed to the activation of preexisting latent pathways originating from spared contralateral bulbospinal axons that decussate at the phrenic nucleus level and terminate monosynaptically on phrenic motoneurons (i.e. crossed phrenic phenomenon, CPP) (Goshgarian, 2003, 2009; Lane et al., 2008; Vinit et al., 2007). If up-regulation of Akt activity is due to a global cellular metabolic demand in the medullary respiratory network, as supported by the upregulation of P-FKHR found in both spared and injured neurons, and, since infusion of LY294002 into the 4th ventricle did not affect P-Akt levels in the cervical spinal cord but would affect both bilateral medullary premotor nuclei contents, it is then likely that such pharmacological inhibition might have affected this contralateral plasticity mechanism at the supraspinal level.

Secondly, it has been shown that PI3K/Akt and FKHR are downstream targets of neurotrophins, including BDNF (Zheng et al., 2002). In the context of the respiratory motor network, BDNF and Akt have been described as key regulatory molecules of respiratory network plasticity during ventilatory challenge, as shown in the case of phrenic long-term facilitation induced in conditions of acute intermittent hypoxia (Baker-Herman et al., 2004; Fuller et al., 2001; Satriotomo et al., 2012). In this case, BDNF is secreted from serotonergic terminals that contact the phrenic motoneuron pool (Baker-Herman et al., 2004). After SCI, the ipsilateral phrenic nucleus of chronic hemisectioned rats is characterized by an increased number of serotonergic terminals, an increased number and length of synaptic active zones per terminal (glutamatergic and serotonergic ones) (Tai and Goshgarian, 1996; Tai et al., 1997), together with an upregulation of BDNF at the spinal level (Li et al., 2007). Thus, at the spinal level, BDNF influences the plasticity of the respiratory network after SCI (Mantilla et al., 2013; Sieck and Mantilla, 2009). At the supraspinal level, we previously found that BDNF was up-regulated in the medulla of SCI rats, suggesting its involvement in plasticity after injury (Felix et al., 2012). Finally, SCI studies focused on the enhancement of axonal outgrowth demonstrated that supraspinal infusion of BDNF in the vicinity of the cell bodies of

injured axons promotes post-lesional plasticity (Bregman et al., 1997; Giehl and Tetzlaff, 1996; Kobayashi et al., 1997; Plunet et al., 2002; Vavrek et al., 2006). Thus, after injury, it is reasonably possible that the same mechanism of plasticity acting through BDNF might coexist at the cervical spinal cord and medulla levels (Fig. 8) to facilitate spontaneous recovery of the respiratory function.

Thirdly, if Akt is primarily involved in plasticity rather than in neuroprotection, through FKHR phosphorylation, then it would mean that FKHR inactivation might be a residual downstream result of Akt activation, a hypothesis which could be supported by the results found in Fig. 2 where FKHR activity is still down-regulated at 90 dpi suggesting that endogenous neuroprotective mechanism might be trivial at this time post-injury. Directly blocking phosphorylation of FKHR would be an interesting follow-up study in order to specifically link this transcription factor with plasticity.

It would have been interesting to evaluate the diaphragm activity after stopping the pharmacological treatment to check whether or not recovery occurs. If recovery occurs, then it would probably mean that the drug transiently inhibits intrinsic plasticity mechanisms that are still active after the period of 21 days or that have the capacity to be expressed thereafter. In line with this hypothesis, we previously found that one potential upstream activator of Akt, BDNF, is still up-regulated in the medulla in chronic conditions after SCI (Felix et al., 2012). Alternatively, a lack of recovery would mean that the acute and subacute phases after SCI are critical periods for post-lesional recovery after which plasticity declines with time. Thus in this case drug would induce irreversible changes. Such a critical period of increased neuronal plasticity has been described after stroke and appears to be during the first fifteen days after brain insult (Biernaskie et al., 2004).

If diaphragmatic spontaneous recovery is prevented under such inhibitory treatment, the weak EMG bursts that could be detected at 21 dpi indicate that the recovery is not completely abolished. Likely explanations include the fact that other cell-signaling pathways may participate in the recovery and that our strategy was not comprehensive enough to completely block the injury-induced activation of PI3K/Akt. For several reasons, we can exclude the possibility that medullary side effects of the LY294002 compound on the respiratory central pattern generator may be responsible for preventing the spontaneous respiratory recovery after SCI. Indeed, such drug treatment has no effect either on baseline respiratory frequency, or the chemoreflex response (as revealed by the reactivity of the respiratory system to respond to ventilatory challenge such as progressive hypercapnia and acute asphyxia); nor on animal weight.

In conclusion, this study demonstrates for the first time that the time-dependent spontaneous respiratory recovery occurring after incomplete cervical hemisection involves a strong intrinsic contribution of the medulla oblongata, through the activation of the PI3K/Akt signaling pathway (Fig. 8). Clarification of the cellular and molecular mechanisms in these supraspinal structures will lead to a deeper understanding of the strategy for functional spontaneous recovery and will open new trails to test therapeutic hypotheses.

Supplementary data to this article can be found online at <http://dx.doi.org/10.1016/j.nbd.2014.05.022>.

#### Author contribution

VM conceived the experiments; MSF, SB, FD, AK, PG, VM performed the experiments; MSF, SB, FD, AK, PG, VM analyzed the data and MSF, SB, FD, FM, AK, PG, VM wrote the manuscript.

#### Acknowledgments

MS Félix and F. Darlot were supported by a PhD fellowship from the French Ministry for Research and Technology. We are grateful to Pr Keith Dudley and Pr Claudio Rivera (INMED, Aix-Marseille University, France) for the manuscript corrections and comments. This work was

supported by Centre National de la Recherche Scientifique (CNRS, #2009–2011, France), Institut National de la Santé et de la Recherche Médicale (INSERM, #2012–2013, France) and Institut pour la Recherche sur la Moelle épinière et l'Encéphale (IRME, #2009–2011, France). The authors declare no competing financial interests.

## References

- Aberg, M.A., Aberg, N.D., Palmer, T.D., Alborn, A.M., Carlsson-Skewir, C., Bang, P., Rosengren, L.E., Olsson, T., Gage, F.H., Eriksson, P.S., 2003. IGF-1 has a direct proliferative effect in adult hippocampal progenitor cells. *Mol. Cell. Neurosci.* 24, 23–40.
- Anderson, K.D., Gunawan, A., Steward, O., 2005. Quantitative assessment of forelimb motor function after cervical spinal cord injury in rats: relationship to the corticospinal tract. *Exp. Neurol.* 194, 161–174.
- Baker-Herman, T.L., Fuller, D.D., Bavis, R.W., Zabka, A.G., Golder, F.J., Doperalski, N.J., Johnson, R.A., Watters, J.J., Mitchell, G.S., 2004. BDNF is necessary and sufficient for spinal respiratory plasticity following intermittent hypoxia. *Nat. Neurosci.* 7, 48–55.
- Ballermann, M., Fouad, K., 2006. Spontaneous locomotor recovery in spinal cord injured rats is accompanied by anatomical plasticity of reticulospinal fibers. *Eur. J. Neurosci.* 23, 1988–1996.
- Bareyre, F.M., Kerschensteiner, M., Raineteau, O., Mettenleiter, T.C., Weinmann, O., Schwab, M.E., 2004. The injured spinal cord spontaneously forms a new intraspinal circuit in adult rats. *Nat. Neurosci.* 7, 269–277.
- Baussart, B., Stamegna, J.C., Polentes, J., Tadie, M., Gauthier, P., 2006. A new model of upper cervical spinal contusion inducing a persistent unilateral diaphragmatic deficit in the adult rat. *Neurobiol. Dis.* 22, 562–574.
- Biernaskie, J., Chernenko, G., Corbett, D., 2004. Efficacy of rehabilitative experience declines with time after focal ischemic brain injury. *J. Neurosci.* 24, 1245–1254.
- Boulenguez, P., Gauthier, P., Kastner, A., 2007. Respiratory neuron subpopulations and pathways potentially involved in the reactivation of phrenic motoneurons after C2 hemisection. *Brain Res.* 1148, 96–104.
- Brazil, D.P., Yang, Z.Z., Hemmings, B.A., 2004. Advances in protein kinase B signalling: AKTion on multiple fronts. *Trends Biochem. Sci.* 29, 233–242.
- Bregman, B.S., McAtee, M., Dai, H.N., Kuhn, P.L., 1997. Neurotrophic factors increase axonal growth after spinal cord injury and transplantation in the adult rat. *Exp. Neurol.* 148, 475–494.
- Bruel-Jungerman, E., Veyrac, A., Dufour, F., Horwood, J., Laroche, S., Davis, S., 2009. Inhibition of PI3K-Akt signaling blocks exercise-mediated enhancement of adult neurogenesis and synaptic plasticity in the dentate gyrus. *PLoS ONE* 4, e7901.
- Brunet, A., Bonni, A., Zigmond, M.J., Lin, M.Z., Juo, P., Hu, L.S., Anderson, M.J., Arden, K.C., Blenis, J., Greenberg, M.E., 1999. Akt promotes cell survival by phosphorylating and inhibiting a Forkhead transcription factor. *Cell* 96, 857–868.
- Burgering, B.M., Kops, G.J., 2002. Cell cycle and death control: long live Forkheads. *Trends Biochem. Sci.* 27, 352–360.
- Dale, E.A., Satriotomo, I., Mitchell, G.S., 2012. Cervical spinal erythropoietin induces phrenic motor facilitation via extracellular signal-regulated protein kinase and Akt signaling. *J. Neurosci.* 32, 5973–5983.
- Darlot, F., Cayetanot, F., Gauthier, P., Matarazzo, V., Kastner, A., 2012. Extensive respiratory plasticity after cervical spinal cord injury in rats: axonal sprouting and rerouting of ventrolateral bulbospinal pathways. *Exp. Neurol.* 236, 88–102.
- Dudek, H., Datta, S.R., Franke, T.F., Birnbaum, M.J., Yao, R., Cooper, G.M., Segal, R.A., Kaplan, D.R., Greenberg, M.E., 1997. Regulation of neuronal survival by the serine–threonine protein kinase Akt. *Science* 275, 661–665.
- Felix, M.S., Popa, N., Djelloul, M., Boucraut, J., Gauthier, P., Bauer, S., Matarazzo, V.A., 2012. Alteration of forebrain neurogenesis after cervical spinal cord injury in the adult rat. *Front. Neurosci.* 6, 45.
- Fuller, D.D., Zabka, A.G., Baker, T.L., Mitchell, G.S., 2001. Phrenic long-term facilitation requires 5-HT receptor activation during but not following episodic hypoxia. *J. Appl. Physiol.* 90, 2001–2006.
- Fuller, D.D., Doperalski, N.J., Dougherty, B.J., Sandhu, M.S., Bolser, D.C., Reier, P.J., 2008. Modest spontaneous recovery of ventilation following chronic high cervical hemisection in rats. *Exp. Neurol.* 211, 97–106.
- Gauthier, P., Baussart, B., Stamegna, J.C., Tadie, M., Vinit, S., 2006. Diaphragm recovery by laryngeal innervation after bilateral phrenicotomy or complete C2 spinal section in rats. *Neurobiol. Dis.* 24, 53–66.
- Ghosh, A., Haiss, F., Sydekum, E., Schneider, R., Gullo, M., Wyss, M.T., Mueggler, T., Baltes, C., Rudin, M., Weber, B., Schwab, M.E., 2010. Rewiring of hindlimb corticospinal neurons after spinal cord injury. *Nat. Neurosci.* 13, 97–104.
- Giehl, K.M., Tetzlaff, W., 1996. BDNF and NT-3, but not NGF, prevent axotomy-induced death of rat corticospinal neurons in vivo. *Eur. J. Neurosci.* 8, 1167–1175.
- Goshgarian, H.G., 2003. The crossed phrenic phenomenon: a model for plasticity in the respiratory pathways following spinal cord injury. *J. Appl. Physiol.* 94, 795–810.
- Goshgarian, H.G., 2009. The crossed phrenic phenomenon and recovery of function following spinal cord injury. *Respir. Physiol. Neurobiol.* 169, 85–93.
- Horwood, J.M., Dufour, F., Laroche, S., Davis, S., 2006. Signalling mechanisms mediated by the phosphoinositide 3-kinase/Akt cascade in synaptic plasticity and memory in the rat. *Eur. J. Neurosci.* 23, 3375–3384.
- Hulsebosch, C.E., 2002. Recent advances in pathophysiology and treatment of spinal cord injury. *Adv. Physiol. Educ.* 26, 238–255.
- Kobayashi, N.R., Fan, D.P., Giehl, K.M., Bedard, A.M., Wiegand, S.J., Tetzlaff, W., 1997. BDNF and NT-4/5 prevent atrophy of rat rubrospinal neurons after cervical axotomy, stimulate GAP-43 and Talpa1-tubulin mRNA expression, and promote axonal regeneration. *J. Neurosci.* 17, 9583–9595.
- Krassioukov, A., 2009. Autonomic function following cervical spinal cord injury. *Respir. Physiol. Neurobiol.* 169, 157–164.
- Kyoto, A., Hata, K., Yamashita, T., 2007. Synapse formation of the cortico-spinal axons is enhanced by RGMa inhibition after spinal cord injury. *Brain Res.* 1186, 74–86.
- Lane, M.A., Fuller, D.D., White, T.E., Reier, P.J., 2008. Respiratory neuroplasticity and cervical spinal cord injury: translational perspectives. *Trends Neurosci.* 31, 538–547.
- Lane, M.A., Lee, K.Z., Fuller, D.D., Reier, P.J., 2009. Spinal circuitry and respiratory recovery following spinal cord injury. *Respir. Physiol. Neurobiol.* 169, 123–132.
- Li, X.L., Zhang, W., Zhou, X., Wang, X.Y., Zhang, H.T., Qin, D.X., Zhang, H., Li, Q., Li, M., Wang, T.H., 2007. Temporal changes in the expression of some neurotrophins in spinal cord transected adult rats. *Neuropeptides* 41, 135–143.
- Mantilla, C.B., Gransee, H.M., Zhan, W.Z., Sieck, G.C., 2013. Motoneuron BDNF/TrkB signaling enhances functional recovery after cervical spinal cord injury. *Exp. Neurol.* 247, 101–109.
- National Research Council (US) Committee, 2011. Guide for the Care and Use of Laboratory Animals, 8th edition. Washington (DC).
- Nishimura, Y., Isa, T., 2009. Compensatory changes at the cerebral cortical level after spinal cord injury. *Neuroscientist* 15, 436–444.
- Nishimura, Y., Isa, T., 2012. Cortical and subcortical compensatory mechanisms after spinal cord injury in monkeys. *Exp. Neurol.* 235, 152–161.
- Noshita, N., Lewen, A., Sugawara, T., Chan, P.H., 2002. Akt phosphorylation and neuronal survival after traumatic brain injury in mice. *Neurobiol. Dis.* 9, 294–304.
- Paterniti, I., Esposito, E., Mazon, E., Bramanti, P., Cuzzocrea, S., 2011. Evidence for the role of PI(3)-kinase-AKT-eNOS signalling pathway in secondary inflammatory process after spinal cord compression injury in mice. *Eur. J. Neurosci.* 33, 1411–1420.
- Plunet, W., Kwon, B.K., Tetzlaff, W., 2002. Promoting axonal regeneration in the central nervous system by enhancing the cell body response to axotomy. *J. Neurosci. Res.* 68, 1–6.
- Polentes, J., Stamegna, J.C., Nieto-Sampedro, M., Gauthier, P., 2004. Phrenic rehabilitation and diaphragm recovery after cervical injury and transplantation of olfactory ensheathing cells. *Neurobiol. Dis.* 16, 638–653.
- Raineteau, O., Schwab, M.E., 2001. Plasticity of motor systems after incomplete spinal cord injury. *Nat. Rev. Neurosci.* 2, 263–273.
- Reimer, M.M., Norris, A., Ohnmacht, J., Patani, R., Zhong, Z., Dias, T.B., Kuscha, V., Scott, A.L., Chen, Y.C., Rozov, S., Frazer, S.L., Wyatt, C., Higashijima, S., Patton, E.E., Panula, P., Chandran, S., Becker, T., Becker, C.G., 2013. Dopamine from the brain promotes spinal motor neuron generation during development and adult regeneration. *Dev. Cell* 25, 478–491.
- Rossignol, S., Frigon, A., 2011. Recovery of locomotion after spinal cord injury: some facts and mechanisms. *Annu. Rev. Neurosci.* 34, 413–440.
- Rossignol, S., Barriere, G., Frigon, A., Barthelemy, D., Bouyer, L., Provencher, J., Leblond, H., Bernard, G., 2008. Plasticity of locomotor sensorimotor interactions after peripheral and/or spinal lesions. *Brain Res. Rev.* 57, 228–240.
- Sabelstrom, H., Stenudd, M., Reu, P., Dias, D.O., Elfineh, M., Zdunek, S., Damberg, P., Goritz, C., Frisen, J., 2013. Resident neural stem cells restrict tissue damage and neuronal loss after spinal cord injury in mice. *Science* 342, 637–640.
- Satriotomo, I., Dale, E.A., Dahlberg, J.M., Mitchell, G.S., 2012. Repetitive acute intermittent hypoxia increases expression of proteins associated with plasticity in the phrenic motor nucleus. *Exp. Neurol.* 237, 103–115.
- Sieck, G.C., Mantilla, C.B., 2009. Role of neurotrophins in recovery of phrenic motor function following spinal cord injury. *Respir. Physiol. Neurobiol.* 169, 218–225.
- Steward, O., Zheng, B., Tessier-Lavigne, M., Hofstadter, M., Sharp, K., Yee, K.M., 2008. Regenerative growth of corticospinal tract axons via the ventral column after spinal cord injury in mice. *J. Neurosci.* 28, 6836–6847.
- Tai, Q., Goshgarian, H.G., 1996. Ultrastructural quantitative analysis of glutamatergic and GABAergic synaptic terminals in the phrenic nucleus after spinal cord injury. *J. Comp. Neurol.* 372, 343–355.
- Tai, Q., Palazzolo, K.L., Goshgarian, H.G., 1997. Synaptic plasticity of 5-hydroxytryptamine-immunoreactive terminals in the phrenic nucleus following spinal cord injury: a quantitative electron microscopic analysis. *J. Comp. Neurol.* 386, 613–624.
- Vavrek, R., Girgis, J., Tetzlaff, W., Hiebert, G.W., Fouad, K., Yee, K.M., 2006. BDNF promotes connections of corticospinal neurons onto spared descending interneurons in spinal cord injured rats. *Brain* 129, 1534–1545.
- Vinit, S., Kastner, A., 2009. Descending bulbospinal pathways and recovery of respiratory motor function following spinal cord injury. *Respir. Physiol. Neurobiol.* 169, 115–122.
- Vinit, S., Boulenguez, P., Efthimiadi, L., Stamegna, J.C., Gauthier, P., Kastner, A., 2005. Axotomized bulbospinal neurons express c-Jun after cervical spinal cord injury. *Neuroreport* 16, 1535–1539.
- Vinit, S., Gauthier, P., Stamegna, J.C., Kastner, A., 2006. High cervical lateral spinal cord injury results in long-term ipsilateral hemidiaphragm paralysis. *J. Neurotrauma* 23, 1137–1146.
- Vinit, S., Stamegna, J.C., Boulenguez, P., Gauthier, P., Kastner, A., 2007. Restorative respiratory pathways after partial cervical spinal cord injury: role of ipsilateral phrenic afferents. *Eur. J. Neurosci.* 25, 3551–3560.
- Vinit, S., Darlot, F., Stamegna, J.C., Sanchez, P., Gauthier, P., Kastner, A., 2008. Long-term reorganization of respiratory pathways after partial cervical spinal cord injury. *Eur. J. Neurosci.* 27, 897–908.

- Vinit, S., Darlot, F., Aoulaiche, H., Boulenguez, P., Kastner, A., 2011. Distinct expression of c-Jun and HSP27 in axotomized and spared bulbospinal neurons after cervical spinal cord injury. *J. Mol. Neurosci.* 45, 119–133.
- Vlahos, C.J., Matter, W.F., Hui, K.Y., Brown, R.F., 1994. A specific inhibitor of phosphatidylinositol 3-kinase, 2-(4-morpholinyl)-8-phenyl-4H-1-benzopyran-4-one (LY294002). *J. Biol. Chem.* 269, 5241–5248.
- Yu, F., Sugawara, T., Maier, C.M., Hsieh, L.B., Chan, P.H., 2005. Akt/Bad signaling and motor neuron survival after spinal cord injury. *Neurobiol. Dis.* 20, 491–499.
- Zhan, L., Li, D., Liang, D., Wu, B., Zhu, P., Wang, Y., Sun, W., Xu, E., 2012. Activation of Akt/FoxO and inactivation of MEK/ERK pathways contribute to induction of neuroprotection against transient global cerebral ischemia by delayed hypoxic postconditioning in adult rats. *Neuropharmacology* 63, 873–882.
- Zhao, H., Shimohata, T., Wang, J.Q., Sun, G., Schaal, D.W., Sapolsky, R.M., Steinberg, G. K., 2005. Akt contributes to neuroprotection by hypothermia against cerebral ischemia in rats. *J. Neurosci.* 25, 9794–9806.
- Zheng, W.H., Kar, S., Quirion, R., 2002. FKHRL1 and its homologs are new targets of nerve growth factor Trk receptor signaling. *J. Neurochem.* 80, 1049–1061.